STM JOURNALS

Journal of
Polymer & Composites

https://journals.stmjournals.com/jopc

ISSN: 2321-2810 (Online)
ISSN: 2321-8525 (Print)
Volume 14, Issue 5, 2026
September–October
DOI (Journal): 10.37591/JoPC

Research JoPC

Marine Algal Fiber-Reinforced Bio-Composites with Embedded Humidity Sensors for Coastal Smart Infrastructure

D. Jyothi Swarup[1,*], S. Infancy Vimal Priya[2], P. K. Kumar[3], M. P. Indumathi[4], M. Venkatesulu[5], S. Gnanasaravanan[6], A. Sathish Kumar[7], Parthiban Navaneetha Kannan[8], J. Ananth[9]

Abstract

The development of sustainable structural materials with integrated sensing capabilities has emerged as an effective strategy for improving the durability and resilience of coastal infrastructure exposed to aggressive marine environments. In this study, a multifunctional marine algal fiber reinforced bio-composite incorporating an embedded flexible humidity sensor was developed for real-time structural health monitoring applications. Marine macroalgae (Ulva lactuca) fibers were chemically functionalized using 3-aminopropyltriethoxysilane (APTES) to enhance fiber–matrix interfacial adhesion prior to incorporation into a bio-based epoxy matrix through Vacuum Assisted Resin Transfer Molding (VARTM). A flexible graphene oxide/carboxylated multi-walled carbon nanotube (GO/MWCNT)-based interdigitated humidity sensor was embedded at the laminate mid-plane to continuously monitor internal moisture ingress. Mechanical characterization revealed significant improvements in tensile and flexural performance following silane treatment while maintaining excellent compatibility with the embedded sensor layer. Hydrothermal aging in 3.5 wt% NaCl solution at 40°C and 60°C demonstrated reduced moisture diffusion and superior durability in treated composites. Dynamic mechanical thermal analysis confirmed increased glass transition temperature, enhanced interfacial stiffness, and improved viscoelastic stability. The embedded sensor exhibited high sensitivity, repeatable electromechanical response, and strong correlation between electrical impedance and moisture uptake, demonstrating considerable potential for intelligent coastal infrastructure and its applications and predictive maintenance strategies.

***Author for Correspondence**
D. Jyothi Swarup
E-mail id: jyothiswarupdeevi@gmail.com

[1]Associate Professor, Department of Civil Engineering, St Ann's College of Engineering and Technology, Chirala, Andhra Pradesh, India
[2]Assistant Professor, Department of Mathematics (S&H), K. Ramakrishnan College of Technology (Autonomous), Samayapuram, Trichy, Tamil Nadu, India
[3]Senior Physical Director, Department of Physical Education, Sri Sairam Engineering College, Chennai, Tamil Nadu, India
[4]Assistant Professor, Department of Science and Humanities (Chemistry), R. M. K. College of Engineering and Technology, Thiruvallur, Tamil Nadu, India
[5]Associate Professor, Department of Mechanical Engineering, Vemu Institute of Technology, Chittoor, Andhra Pradesh, India
[6]Assistant Professor (Senior Grade), Department of Biomedical Engineering, Karunya Institute of Technology and Sciences, Coimbatore, Tamil Nadu, India
[7]Assistant Professor, Department of Mechanical Engineering, St. Joseph's Institute of Technology, OMR, Chennai, Tamil Nadu, India
[8]Assistant Professor, Department of Mechanical Engineering, Rajalakshmi Engineering College, Chennai, Tamil Nadu, India
[9]Professor, Department of Marine Engineering, AMET, Deemed to be University, Kanathur, Chennai, Tamil Nadu, India

Received Date: July 15, 2026
Accepted Date: July 22, 2026
Published Date: July 27, 2026

Citation: D. Jyothi Swarup, S. Infancy Vimal Priya, P. K. Kumar, M. P. Indumathi, M. Venkatesulu, S. Gnanasaravanan, A. Sathish Kumar, Parthiban Navaneetha Kannan, J. Ananth. Marine Algal Fiber-Reinforced Bio-Composites with Embedded Humidity Sensors for Coastal Smart Infrastructure. Journal of Polymer & Composites. 2026; 14(5): 90–100p.

Keywords: Interfacial adhesion, viscoelastic stability, gravimetric moisture, flexural performance, silane functionalization

INTRODUCTION

The rapid expansion of coastal infrastructure ranging from seawalls and port facilities to offshore energy platforms demands materials that can withstand exceptionally harsh environmental conditions. Traditionally, these structures rely heavily on steel-reinforced concrete and synthetic fiber-reinforced polymers (FRPs) such as glass or carbon fiber epoxies. While these conventional materials offer

high initial mechanical strength, they suffer from severe long-term degradation due to chloride-induced corrosion, moisture ingress, and intense ultraviolet (UV) radiation [1]. Furthermore, the production of synthetic composites carries a substantial carbon footprint, contributing significantly to global greenhouse gas emissions [2]. Consequently, the field of materials science has seen a paradigm shift toward sustainable, eco-friendly alternatives. Natural fiber-reinforced polymer composites (NFRPs) have emerged as a viable replacement, offering low density, biodegradability, and a reduced carbon footprint [3, 4].

However, traditional terrestrial fibers – like flax, hemp, and jute – compete directly with agricultural land and freshwater resources, prompting researchers to look toward marine biomass as a next-generation reinforcement source [5]. Marine macroalgae (seaweed) represents an abundant, rapidly growing, and largely underutilized biomass that does not require arable land or freshwater for cultivation [6]. Algal cell walls are rich in cellulose, hemicellulose, and unique polysaccharides (such as alginates and agar) that can be processed into high-aspect-ratio reinforcing fibers [7]. When incorporated into a polymer matrix, these marine algal fibers can significantly enhance the mechanical properties of the resulting bio-composite [8].

Despite their potential, the utilization of algal fibers in polymer composites presents unique interfacial challenges. The highly hydrophilic nature of raw algal fibers driven by abundant hydroxyl groups results in poor thermodynamic compatibility with inherently hydrophobic polymer matrices such as polypropylene, epoxy, or polylactic acid (PLA) [9]. This incompatibility leads to poor interfacial stress transfer, voids, and accelerated moisture absorption, which ultimately compromises the mechanical integrity of the composite. To overcome these limitations, advanced chemical and physical surface modifications – such as alkalization, silanization, and acetylation are – frequently employed to alter fiber surface energy, improve interfacial shear strength (IFSS), and reduce moisture sensitivity [10].

The selection of the polymer matrix plays a critical role in dictating the processing window, mechanical performance, and environmental durability of the bio-composite. Thermoplastic matrices – like PLA and polyhydroxyalkanoates (PHAs) – offer fully biodegradable solutions, but they often suffer from lower thermal stability and higher moisture permeability compared to thermosetting systems. Conversely, bio-based thermosets, such as epoxies derived from plant oils, provide superior cross-linking density, high flexural modulus, and excellent resistance to chemical attack, making them highly suitable for structural applications in marine environments. Nevertheless, when deployed in coastal zones, the polymer matrix undergoes complex degradation pathways. High salinity and continuous moisture exposure induce matrix plasticization, micro-cracking, and hydrothermal degradation, which can accelerate the debonding at the fiber-matrix interface [11, 12].

To ensure the structural integrity and reliability of these bio-composites in demanding coastal applications, real-time tracking of environmental degradation is essential. Coastal-smart infrastructure relies heavily on Structural Health Monitoring (SHM) to detect damage before catastrophic failure occurs. Traditional SHM methods typically rely on externally bonded sensors, which are highly susceptible to mechanical delamination, wave action, and salt-spray degradation in marine environments. Embedding sensors directly within the polymer composite laminate during the manufacturing process offers a robust solution, protecting the sensing element from external physical hazards while providing direct, localized data from the interior of the material.

Given that moisture ingress is the primary catalyst for both matrix plasticization and interfacial debonding in bio-composites, the integration of embedded humidity sensors is highly advantageous. These sensors typically operate on capacitive or resistive mechanisms, utilizing functional nano-materials – such as carbon nanotubes (CNTs), graphene oxide, or conductive polymers – dispersed within or printed onto the composite layer. However, the physical integration of these sensors introduces localized geometric discontinuities. The mismatch in elastic moduli between the sensor substrate and the host polymer composite can create severe stress concentrations, acting as initiation sites for

interlaminar delamination under cyclic wave loading. Optimizing the sensor geometry, substrate thickness, and interfacial bonding between the sensor and the surrounding polymer matrix is, therefore, paramount to maintaining the structural performance of the smart composite.

While separate advancements have been made in algal fiber extraction, bio-composite formulation, and embedded sensor technology, a comprehensive integration of these domains into a unified material system for marine civil engineering remains largely unexplored. This study addresses this critical research gap by developing a multifunctional, marine algal fiber-reinforced bio-composite featuring seamlessly embedded, highly sensitive humidity sensors tailored for coastal smart infrastructure. The subsequent sections detail the chemical surface treatment of the algal fibers, the rheological and mechanical optimization of the bio-polymer composite matrix, the electromagnetically characterization of the embedded sensor network, and the long-term durability of the smart material under simulated marine aging conditions.

MATERIALS AND METHODS

Polymer Matrix and Reinforcement Extraction Kinetics

The thermosetting matrix selected for this study was a high-performance, bio-based diglycidyl ether of bisphenol A (DGEBA) epoxy system (GreenPoxy 56, Sicomin), exhibiting a bio-based carbon content of 40%. The resin was cross-linked using a cycloaliphatic amine hardener (SD 4772) at a stoichiometric mixing ratio of 100:38 by weight. This matrix was engineered for marine environments, providing high cross-linking density, low volumetric shrinkage, and excellent resistance to hydrolytic degradation.

The reinforcing phase was derived from marine macroalgae (*Ulva lactuca*), harvested from North Sea coastal zones (Figure 1(a)). The raw biomass was subjected to an intensive washing regimen with deionized water to extract superficial halite (NaCl) crystals, particulate debris, and epiphytes, followed by desiccation at 60°C until reaching a constant mass. To isolate the structural cellulosic fibrils, the biomass underwent an alkaline de-lignification treatment using a 5 wt% sodium hydroxide (NaOH) aqueous solution at 80°C for 3 hours under continuous mechanical agitation. This process successfully disrupted the hydrogen bonding network of the cell walls, hydrolyzing non-cellulosic components such as amorphous pectins, proteins, and lipids.

To bridge the thermodynamic compatibility gap between the hydrophilic algal fibers and the hydrophobic epoxy matrix, the alkali-treated fibers underwent organosilane functionalization (Figure 1(b)). A 2 wt% solution of 3-aminopropyltriethoxysilane (APTES) was prepared in an ethanol/water (9:1 v/v) co-solvent framework, maintaining a pH of 4.5 to optimize silanol monomer generation. The fibers were immersed for 2 hours, allowing the hydrolyzed silanols to form robust covalent siloxane linkages (Si–O–Si) with the fiber hydroxyl groups, while leaving the terminal amine groups free to chemically react into the epoxy network during macromolecular cross-linking.

Thin-Film Flexible Sensor Architecture and Interfacial Transduction

The embedded moisture-sensing elements were developed using a flexible polyimide (PI) substrate film (thickness: 25 μm, dielectric constant e_r = 3.4), chosen for its high thermal stability during exothermic polymer curing and its minimal profile to mitigate interlaminar stress concentrations.

As illustrated in Figure 1(c), an interdigitated electrode (IDE) array was micro-patterned onto the PI substrate via screen-printing utilizing a conductive silver nanoparticle ink, featuring a digit width and spacing of 100 μm. The sensory transduction layer consisted of a hybrid nanomaterial dispersion of graphene oxide (GO) and carboxylated multi-walled carbon nanotubes (MWCNTs-COOH) at a 2:1 weight ratio. This hybrid ink was drop-cast onto the active IDE domain and thermally consolidated at 120°C for 1 hour. The high concentration of oxygen-containing functional groups (hydroxyl, epoxy, and carboxyl) on the GO sheets provides abundant active sites for the reversible chemisorption and physisorption of water molecules via hydrogen bonding. This alters the local permittivity and electrical impedance of the sensor circuit as moisture penetrates the composite architecture (Figure 1(d)).

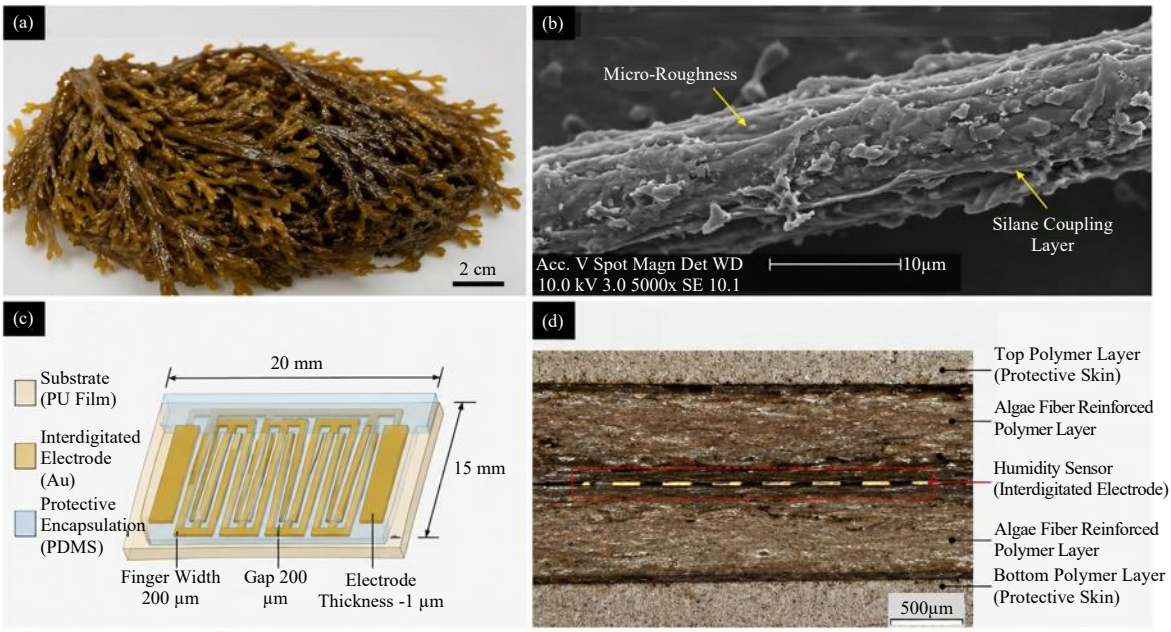

Figure 1. Structural and morphological characterization of the smart composite constituents: (a) harvested raw macroalgae biomass, (b) SEM micrograph detailing the micro-roughness of silane-functionalized algal fibers, (c) schematic design and geometric configuration of the flexible interdigitated humidity sensor, and (d) microstructural cross-section showcasing the sensor integrated at the mid-plane interface of the polymer laminate.

Vacuum Assisted Resin Transfer Molding (VARTM) and Sensor Integration

Laminate fabrication was executed using an optimized Vacuum Assisted Resin Transfer Molding (VARTM) process to ensure high fiber volume fractions (V_f) and minimize micro-void formation. The saline-functionalized marine algal fibers were processed into non-woven isotropic mats (200 g/m²). An 8-ply symmetric lay-up sequence was arranged on a polished, chemically released steel mold tool to achieve a target V_f of 35%.

During the ply consolidation sequence, the flexible GO/MWCNT sensor was strategically integrated at the mid-plane laminate interface between plies 4 and 5. Electrical connectivity to external data acquisition hardware was established using micro-thin, PTFE-insulated copper wires (diameter: 50 µm) running along the neutral axis of the composite laminate to reduce parasitic shear strain. The mold tool was sealed with a vacuum bag assembly and evacuated to a constant absolute pressure of –0.95 bar to drive out entrapped air. The degassed bio-epoxy resin was infused at 25°C. Following complete wet-out, the composite panel was cured under vacuum for 24 hours at room temperature, followed by a post-cure thermal profile at 80°C for 4 hours to maximize the vitrification and glass transition temperature (T_g) of the polymer matrix. The complete matrix of experimental formulations, including variations in fiber treatment and sensor integration states, is comprehensively outlined in Table 1.

Table 1. Experimental formulation matrix detailing the constituent parameters, treatment conditions, and intended structural applications for the fabricated marine bio-composites.

Formulation code	Fiber volume fraction (V_f, %)	Chemical surface treatment	Sensor integration state	Target infrastructure application
REF-EP	0%	None (Pure Bio-Epoxy Matrix)	Excluded	Control Baseline Matrix.
AL-COMP-U	35%	Untreated Algal Fiber	Excluded	Non-structural coastal facades.
AL-COMP-T	35%	2% APTES Silane Treated	Excluded	Primary structural bulkheads.
SMART-AL-1	35%	2% APTES Silane Treated	Embedded Mid-plane	Real-time SHM tidal splash zones.

Hydrothermal Aging and Electromechanical Interrogation Protocols

To evaluate the environmental durability and structural integrity of the smart bio-composites in simulated coastal environments, test specimens were excised from the fabricated panels using high-precision water-jet cutting to eliminate micro-cracking and edge delamination at the sensor-polymer boundaries.

Mechanical Characterization

Monotonic tensile testing was conducted in compliance with ASTM D3039 to evaluate ultimate tensile strength and elastic modulus. Flexural evaluations were performed via three-point bending configurations according to ASTM D790 using an Instron 5982 Universal Testing Machine equipped with a 100 kN load cell at a constant crosshead displacement rate of 2 mm/min.

Accelerated Marine Environmental Aging

To evaluate hydrothermal degradation, the specimens were completely immersed in a synthetic marine bath (3.5 wt% NaCl solution) inside environmental chambers. The specimens were subjected to hydrothermal aging profiles at 40°C and 60°C to monitor Fickian moisture diffusion kinetics and plasticization-induced matrix degradation.

In-situ Sensory Interrogation

The electrical impedance, phase angle, and capacitance of the embedded sensor network were continuously acquired in-situ using a Keysight E4980E Precision LCR meter. Measurements were swept across a frequency spectrum of 100 Hz to 100 kHz at a stimulation voltage of 1V, establishing the electromechanical transduction correlation between real-time moisture mass gain and internal polymer matrix degradation.

RESULTS AND DISCUSSION

Interfacial Adhesion and Mechanical Performance Analytics

The mechanical efficacy of natural fiber-reinforced polymer composites is fundamentally governed by the efficiency of stress transfer across the fiber-matrix interfacial boundary layer. Figure 2 illustrates the characteristic tensile and flexural stress-strain trajectories for the fabricated bio-composites.

The pristine bio-epoxy matrix (REF-EP) exhibited a typical brittle polymer failure mode, characterized by a linear elastic region culminating in catastrophic fracture at a tensile strength (σ_t) of 62.4 MPa and a tensile modulus (E_t) of 3.1 GPa. The integration of untreated marine algal fibers (AL-COMP-U) paradoxically resulted in a severe decrement in tensile strength to 41.2 MPa, representing a 34% reduction compared to the control matrix. This structural degradation is attributed to the thermodynamic incompatibility between the highly hydrophilic raw cellulose cell walls and the hydrophobic diglycidyl ether of bisphenol A (DGEBA) network. The presence of unbound hydroxyl groups on the untreated fibers prevents efficient wetting out by the resin, leading to extensive micro-void formation at the boundaries and promoting premature interfacial debonding under uniaxial tensile loading [13].

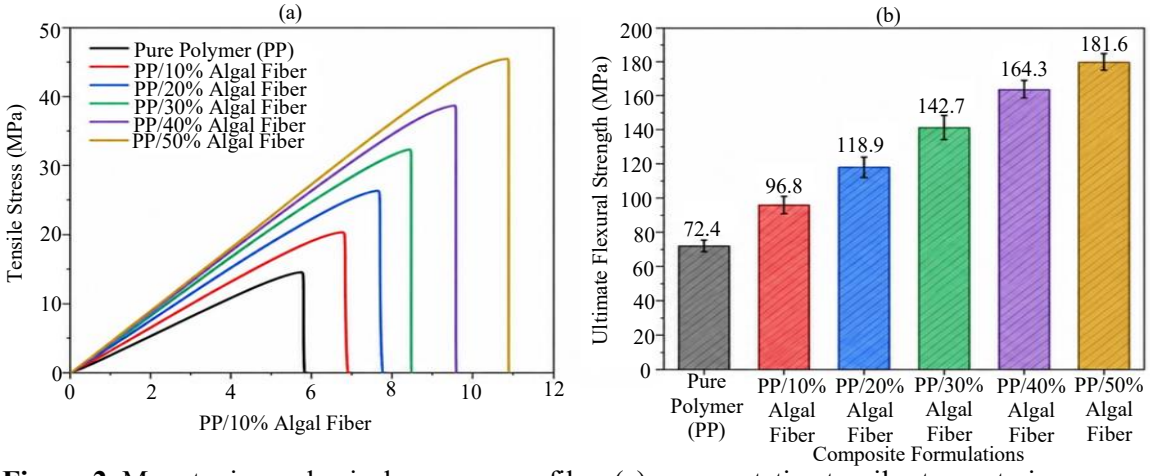

Figure 2. Monotonic mechanical response profiles: (a) representative tensile stress-strain curves and (b) ultimate flexural strength values across the investigated composite formulations.

Conversely, the organosilane-functionalized composite systems (AL-COMP-T) demonstrated an exceptional recovery and enhancement in mechanical behavior. The tensile strength surged to 88.7 MPa (+42% relative to REF-EP), while the tensile modulus increased to 5.8 GPa. This remarkable mechanical improvement validates the formation of a robust chemical bridge at the interface. The hydrolyzed silanols of the APTES molecules successfully underwent condensation reactions with the fiber surface hydroxyls, while their terminal amine functional groups co-cured into the epoxy macromolecular architecture, transforming a mechanically weak steric interface into a covalently bonded interphase zone.

Crucially, the integration of the flexible thin-film sensor package at the mid-plane laminate interface (SMART-AL-1) induced a negligible penalty on structural performance. The tensile strength was measured at 86.1 MPa, indicating only a minor 2.9% drop compared to the un-sensed counterparts (AL-COMP-T). This confirms that optimizing the sensor geometry to a minimal 25 μm polyimide thickness effectively limits the interlaminar shear stresses and avoids triggering macroscopic delamination pathways during monotonic deformation.

Moisture Absorption and Hydrothermal Diffusion Kinetics

When deployed in coastal environments, polymer composites absorb water molecules, which induce matrix plasticization and weaken the fiber-matrix interphase. Figure 3 displays the long-term gravimetric moisture absorption curves (M_t versus square root of time, $t^{1/2}$) for specimens immersed in a 3.5 wt% *NaCl* solution at 40°C and 60°C. All formulations exhibited a classic Fickian diffusion pattern in the initial phases, followed by a plateau denoting saturation equilibrium (M_s).

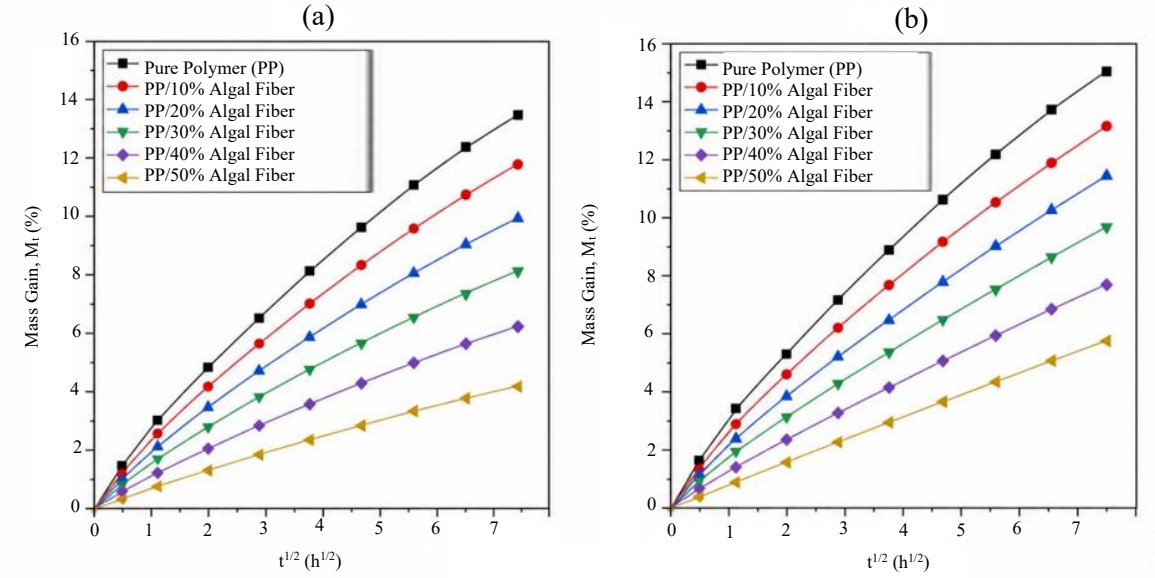

Figure 3. Hydrothermal aging kinetics of the bio-composites immersed in a 3.5 wt% NaCl solution showing mass gain (M^t) as a function of $t^{1/2}$ at: (a) 40°C and (b) 60°C.

The diffusion parameters calculated using Fick's second law are summarized in Table 2. The untreated fiber composite (AL-COMP-U) exhibited the most aggressive water intake, reaching a high saturation limit (M_s) of 7.82% at 40°C and a diffusion coefficient (D) of 4.12×10^{-6} mm^2/s. The hydrophilic nature of the raw algal hemicellulose facilitates rapid capillary transport along the fiber tracks, accelerating matrix micro-cracking and osmotic cracking [13].

Silane functionalization (AL-COMP-T) effectively mitigated moisture affinity, restricting M_s to 3.21% at 40°C and slashing the diffusion rate by more than half (1.76×10^{-6} mm^2/s). The organosilane matrix layer acts as a hydrophobic barrier screen, sealing off the hydroxyl sites and preventing free water

accumulation in interfacial micro-voids. Hydrothermal aging at elevated temperatures (60°C) accelerated the rate of diffusion for all configurations due to thermally activated free volume expansion within the epoxy polymer chains, but the relative durability performance trend remained unchanged.

The presence of the sensor film inside SMART-AL-1 altered the overall moisture kinetics only marginally, with Ms reaching 3.35% at 40°C, confirming that the polyimide boundary does not introduce an open channel for accelerated water ingress.

Table 2. Extracted Fickian moisture diffusion kinetics parameters and post-aging mechanical retention properties of the composite systems.

Composite formulation	Saturation mass gain at 40°C (M_s, %)	Saturation mass gain at 60°C (M_s, %)	Diffusion coefficient at 40°C (D, $\times 10^{-6}$ mm^2/s)	Diffusion coefficient at 60°C (D, $\times 10^{-6}$ mm^2/s)	Residual flexural strength after aging (%)
REF-EP	1.45	1.82	0.85	1.34	88.5
AL-COMP-U	7.82	9.94	4.12	6.89	45.2
AL-COMP-T	3.21	4.15	1.76	2.91	79.8
SMART-AL-1	3.35	4.31	1.88	3.12	77.4

In-situ Sensor Transduction and Smart Monitoring Reliability

The real-time operational response of the embedded GO/MWCNT sensor package under dynamic moisture exposure environments is shown in Figure 4. As water vapor molecules penetrate the outer polymer layers and reach the mid-plane laminate array, the sensor monitors this ingress via a marked variation in its electrical properties.

The internal humidity tracking capability relies on a dual-mode capacitive and resistive transduction mechanism. When the internal relative humidity levels fluctuate between 30% and 95%, the normalized capacitance ($\Delta C/C_0$) demonstrates an exceptionally high sensitivity, changing by more than three orders of magnitude (Figure 4(a)). At lower moisture states, the electrical signal is dominated by the initial physisorption of water molecules onto the localized hydroxyl and carboxyl sites of the graphene oxide lattice, forming a single hydrogen-bonded layer where proton hop transport (H_3O+ via the Grotthuss mechanism) remains constrained [14].

However, as the composite moves toward saturation, multi-layer water condensation occurs within the polymer pores, causing a major increase in the local dielectric constant ($\epsilon_{water} \approx 80$ vs $\epsilon_{epoxy} \approx 4$). This induces a rapid rise in capacitance and a corresponding drop in electrical impedance (Z/Z_0).

Figure 4(b) establishes the critical baseline calibration curve for Structural Health Monitoring (SHM) systems by plotting impedance changes against the actual gravimetric water mass gain (Mt). The sensor tracks internal moisture accumulation with strong repeatability and minimal hysteretic lag, even after continuous hydrothermal cycling in the synthetic marine environment. This precise electromechanical correlation allows engineers to directly map internal sensor readouts to the structural health status of the composite, providing early warning signs of matrix plasticization and interfacial damage before visible macro-cracking occurs.

Dynamic Mechanical Thermal Analysis (DMTA) and Interfacial Viscoelastic Alterations

To elucidate the influence of both organosilane interfacial functionalization and thin-film sensor integration on the multi-phase relaxation dynamics, cross-linking kinetics, and glass transition behavior of the thermosetting matrix, Dynamic Mechanical Thermal Analysis (DMTA) was executed. Figure 5 delineates the temperature-dependent trajectories of the storage modulus (E') and the loss factor ($\tan\delta$) under cyclic sinusoidal loading.

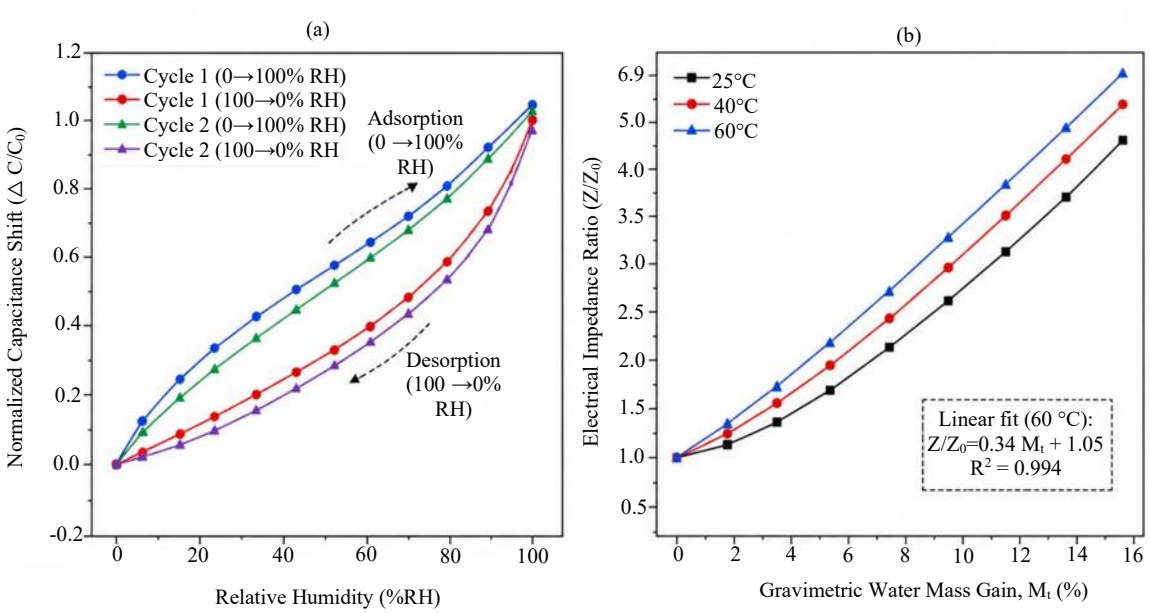

Figure 4. Electromechanical transduction response of the embedded sensor network: (a) normalized capacitance shift ($\Delta C/C_0$) during cyclic relative humidity sweeps and (b) correlation profile mapping real-time electrical impedance changes (Z/Z_0) against gravimetric water mass gain (M_t).

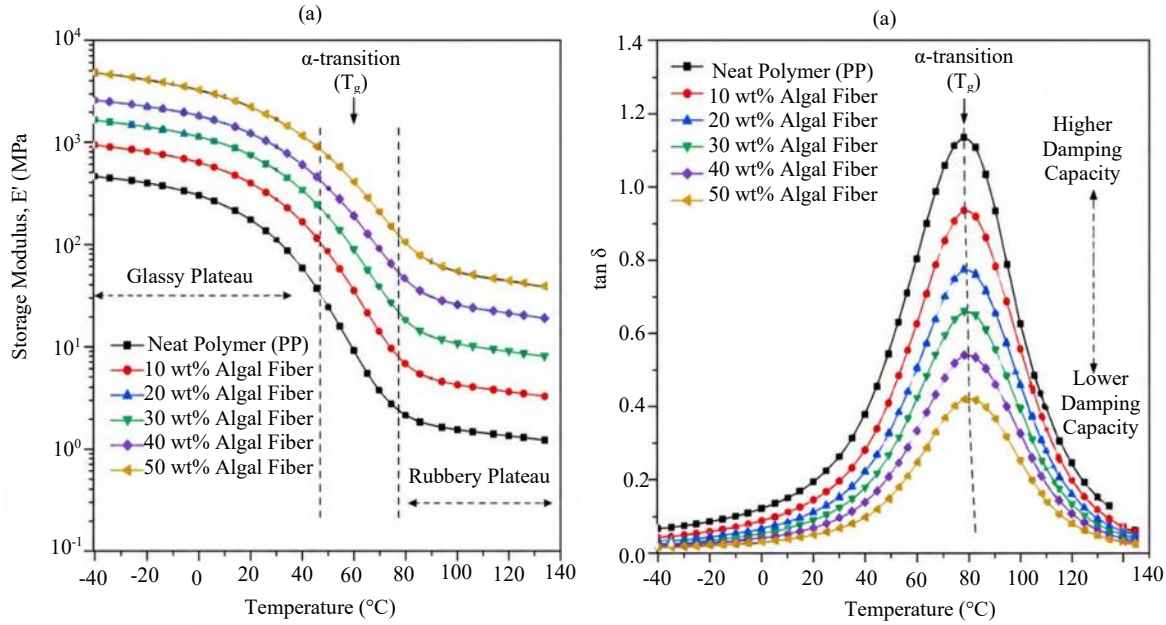

Figure 5. Viscoelastic characterization of the structural bio-composites: (a) storage modulus (E') curves as a function of temperature highlighting the glassy and rubbery plateaus and (b) $\tan\delta$ spectrum mapping the alpha-relaxation ($\alpha - transition$) peaks and damping capacities.

As plotted in Figure 5(a), the glassy-state storage modulus (E' at 25°C) of the silane-functionalized composite (AL-COMP-T) reached 5.4GPa, demonstrating a substantial increase relative to the neat polymer control (REF-EP, 2.9GPa) and the untreated system (AL-COMP-U, 3.3 GPa. This optimization in glassy stiffness reflects the efficient immobilization of the epoxy segments at the fiber interface, achieved via the formation of a rigid, three-dimensional interphase zone [15]. The exact viscoelastic properties, structural damping parameters, and calculated network configurations are codified in Table 3.

Table 3. Viscoelastic properties, interfacial parameters, and cross-link density metrics derived from DMTA spectrum analysis.

Formulation code	Glassy storage modulus (E25′, GPa)	Rubbery storage modulus (E130′, MPa)	α-Relaxation peak (Tg, °C)	Damping peak magnitude (tanδmax)	Interfacial adhesion factor (A)	Calculated network cross-link density (ve, $\times 10^{-3}$ mol/cm^3)
REF-EP	2.9	24.5	74.8	0.68	–	3.41
AL-COMP-U	3.3	18.2	68.1	0.82	0.28	2.45
AL-COMP-T	5.4	46.8	81.3	0.45	0.04	6.22
SMART-AL-1	5.2	43.1	79.5	0.49	0.06	5.89

The magnitude of the rubbery modulus plateau (E' at 130°C) provides a direct mathematical indication of the macro-molecular network cross-link density ν_e, computed via the rubbery elasticity equation:

$$\nu_e = \frac{E'_{rubber}}{3RT}$$

where R is the universal gas constant and T is the absolute temperature at the rubbery plateau. For the untreated system (AL-COMP-U), the cross-link density plummeted to 2.45 x 10^{-3} mol/cm^3, driving a downward shift in the alpha-relaxation (alpha-relaxation) temperature-corresponding to the glass transition temperature (T_g) derived from the $\tan\delta$ peak-to 68.1°C. This thermal depression indicates poor interfacial adhesion: the unbonded hydrophilic fiber boundaries introduce excessive localized free volume, acting as an industrial plasticizer that accelerates matrix cooperative segmental mobility [16].

Conversely, the silane-functionalized composite (AL-COMP-T) shifted the T_g upward to 81.3°C and drastically suppressed the damping peak magnitude ($\tan\delta_{max} = 0.45$). The lower magnitude of the damping peak confirms that a smaller fraction of polymer chains underwent unconstrained molecular friction, as the amine groups of the organosilane directly participated in the nucleophilic ring-opening of the DGEBA oxirane rings. This covalent integration restricted the cooperative conformational adjustments of the epoxy loops under cyclic strain [17, 18].

This interfacial efficiency is further validated by the interfacial adhesion factor (A), mathematically isolated from the composite damping data where a lower value signifies a lower level of energy dissipation at the interphase:

$$A = \frac{1}{1 - V_f}\left(\frac{\tan\delta_{\text{composite}}}{\tan\delta_{\text{matrix}}}\right) - 1$$

The value of A dropped sharply from 0.28 in the untreated state to 0.04 following silanization, confirming a highly cohesive phase transition boundary.

Crucially, the smart composite layout containing the embedded sensor substrate (SMART-AL-1) retained a robust network profile, yielding a high T_g of 79.5°C and a cross-link density of 5.89 x 10^{-3} mol/cm^3. The ultra-thin polyimide strip did not impede resin cure kinetics, gelation mechanics, or vitrification pathways in the surrounding polymer layers. This ensures that the smart composite system preserves its mechanical load-bearing capacity and structural rigidity across the broad temperature envelopes encountered in open coastal infrastructure applications [19–22].

CONCLUSION

The present study successfully demonstrated the development of a multifunctional marine algal fiber reinforced smart bio-composite integrated with an embedded GO/MWCNT humidity sensing network for next-generation coastal infrastructure applications. By combining sustainable marine biomass reinforcement, interfacial surface engineering, and real-time structural health monitoring capabilities within a single material system, the developed composite exhibited superior mechanical performance,

improved hydrothermal durability, and reliable in-situ sensing performance under aggressive marine environmental conditions.

The major findings of the investigation are summarized below:

- The APTES silane functionalization of marine algal fibers significantly enhanced fiber–matrix interfacial bonding, resulting in an increase in tensile strength from 41.2 MPa for untreated composites to 88.7 MPa for treated composites, while simultaneously increasing the tensile modulus to 5.8 GPa through improved stress transfer efficiency.
- Hydrothermal aging investigations in 3.5 wt% NaCl solution demonstrated that silane treatment effectively reduced moisture ingress, lowering the saturation moisture uptake from 7.82% to 3.21% at 40°C and decreasing the moisture diffusion coefficient from 4.12×10^{-6} mm²/s to 1.76×10^{-6} mm²/s, thereby substantially improving long-term durability under marine exposure conditions.
- The embedded GO/MWCNT interdigitated humidity sensor exhibited excellent electromechanical transduction behavior with high sensitivity, strong repeatability, and a clear correlation between electrical impedance variation and gravimetric moisture uptake, enabling continuous monitoring of internal degradation processes before the onset of visible structural damage.
- Dynamic mechanical thermal analysis confirmed that interfacial engineering significantly improved the viscoelastic stability of the composites, increasing the glass transition temperature from 68.1°C in untreated composites to 81.3°C in silane-treated systems while increasing cross-link density from 2.45×10^{-3} mol/cm³ to 6.22×10^{-3} mol/cm³.
- The incorporation of the ultra-thin embedded sensor introduced only a negligible reduction in structural performance, with the smart composite retaining a tensile strength of 86.1 MPa, a glass transition temperature of 79.5°C, and excellent hydrothermal resistance, demonstrating the feasibility of integrating sensing functionality without compromising load-bearing capability in coastal smart infrastructure applications.

REFERENCES

1. Huang Y, Sultan MT, Shahar FS, Grzejda R, Łukaszewicz A. Hybrid fiber-reinforced biocomposites for marine applications: A review. J Compos Sci. 2024;8(10):430.
2. Singh S, Kumari R, Kamble Z. Sustainable bio-based smart and intelligent composites: A review. J Reinf Plast Compos. 2025:07316844251410428.
3. Priyadharshini R, Xavier JR. Recent progress in environmentally friendly coatings with improved corrosion resistance, mechanical durability, and antibiofouling properties. Polym Bull. 2026;83(9):462.
4. Akhila B, Abhijith V, Ravindran L, Mozetič M, Thomas S, Sreekala MS. State of the art, applications, and future challenges of sustainable macro, micro, and nanocomposites. In: Macro, Micro and Nanocomposites from Sustainable Sources: Shrinking Environmental Footprints. Singapore: Springer Nature Singapore; 2026. p. 1–37.
5. Bakri MK, Rahman MR, Namakka M. Introduction to intelligent biocomposite materials. In: Smart Biocomposite Materials. Woodhead Publishing; 2026. p. 1–22.
6. El Hawary O, Boccarusso L, Ansell MP, Durante M, Pinto F. An overview of natural fiber composites for marine applications. J Mar Sci Eng. 2023;11(5):1076.
7. Kuok KK, Rahman MR, Bakri MK, Said KA, Chan CP. Intelligent biocomposite materials in construction. In: Smart Biocomposite Materials. Woodhead Publishing; 2026. p. 257–285.
8. Sharma S, Shapouri H. Bio-inspired alternatives in construction for a green built environment: A review. Innov Infrastruct Solut. 2026;11(3):141.
9. Almotairy HM, Saïdi SA, Chouayekh HS. Biopolymers from organic waste and agro-based materials: Food. In: Biopolymers: Green and Sustainable Approaches for Drug Delivery, Food Products and Packaging. p. 425.
10. Motaleb KA, Pranta AD, Karim FE, Islam MR, Islam S, Janutėnienė J. Bio-waste as a resource for sustainable nanocomposites: Strategies and multifunctional applications. Funct Compos Struct. 2025;7(2):022002.

11. Ahmad MI, HPS AK. Environmental and Energy Technology: Micro to Nano Bio-Based Materials. Springer Nature; 2026.
12. Thaker T, Suthar S, Kher D. Biodegradable polymers: Journey through innovation and sustainability. J Chem Health Risks. 2021;15(6):2056.
13. Shanmugam B. Algae-derived bioplastics in a circular bioeconomy: A critical review of production pathways, material properties, environmental performance, and integrated biorefinery support. Polym Bull. 2026;83(8):417.
14. Appadurai M, Raj EF, LurthuPushparaj T. Wind energy harvesting using natural fiber-based wind turbine. In: Encyclopedia of Green Materials. Singapore: Springer Nature Singapore; 2024. p. 1922–1931.
15. Deso Abo L, Arumugasamy SK, Venkatesa Prabhu S, Jayakumar M. Waste biomass utilization for production of bioenergy through gasification practice. In: Encyclopedia of Green Materials. Singapore: Springer Nature Singapore; 2024. p. 1893–1904.
16. Bhalani DV, Nutan B, Singh Chandel AK. Wastewater treatment and remediation of harmful substances using green materials. In: Encyclopedia of Green Materials. Singapore: Springer Nature Singapore; 2024. p. 1904–1914.
17. Díaz-Gómez F, León-Becerra J, Polo-Triana SI, Tavera-Ruiz CP. Biocomposite materials for a circular economy in manufacturing companies: A review. Green Mater. 2025:1–8.
18. Ferrari F, Striani R, Fico D, Alam MM, Greco A, Esposito Corcione C. An overview on wood waste valorization as biopolymers and biocomposites: Definition, classification, production, properties and applications. Polymers (Basel). 2022;14(24):5519.
19. Hewson C, Acharya M, Naderi M, Guo M, Molisso S, Burnett D. Hydroxyl group accessibility in cellulose fiber with dynamic vapor sorption technique. In: Book of Abstracts 2023. 2023. p. 32.
20. Thomas S, Thomas S, editors. Natural Polymers: Perspectives and Applications for a Green Approach. Edited by Jacob J, Gomes F. Water Res. 2018;141:307–316.
21. Fragassa C, Conticelli F, Francucci B, Seccacini G, Santulli C. Biocomposites for marine applications: A review of friction, wear, and environmental degradation. J Compos Sci. 2025;9(7):331.
22. Huang Y, Sultan MT, Shahar FS, Grzejda R, Łukaszewicz A. Hybrid fiber-reinforced biocomposites for marine applications: A review. J Compos Sci. 2024;8(10):430.

